



## 저작자표시-비영리-변경금지 2.0 대한민국

이용자는 아래의 조건을 따르는 경우에 한하여 자유롭게

- 이 저작물을 복제, 배포, 전송, 전시, 공연 및 방송할 수 있습니다.

다음과 같은 조건을 따라야 합니다:



저작자표시. 귀하는 원저작자를 표시하여야 합니다.



비영리. 귀하는 이 저작물을 영리 목적으로 이용할 수 없습니다.



변경금지. 귀하는 이 저작물을 개작, 변형 또는 가공할 수 없습니다.

- 귀하는, 이 저작물의 재이용이나 배포의 경우, 이 저작물에 적용된 이용허락조건을 명확하게 나타내어야 합니다.
- 저작권자로부터 별도의 허가를 받으면 이러한 조건들은 적용되지 않습니다.

저작권법에 따른 이용자의 권리는 위의 내용에 의하여 영향을 받지 않습니다.

이것은 [이용허락규약\(Legal Code\)](#)을 이해하기 쉽게 요약한 것입니다.

[Disclaimer](#)

공학석사학위논문

사린의 구조 유사물질인 DMMP 감지를 위한  
인간 후각수용체 기반의 CNT-FET 센서

Human olfactory receptor-based CNT-FET sensor for the  
detection of DMMP as a simulant of sarin

2018년 2월

서울대학교 대학원

화학생물공학부

유 진

공학석사학위논문

사린의 구조 유사물질인 DMMP 감지를 위한  
인간 후각수용체 기반의 CNT-FET 센서

Human olfactory receptor-based CNT-FET sensor for the  
detection of DMMP as a simulant of sarin

2018년 2월

서울대학교 대학원

화학생물공학부

유 진

## Abstract

# Human olfactory receptor–based CNT–FET sensor for the detection of DMMP as a simulant of sarin

Jin Yoo

School of Chemical and Biological Engineering

The Graduate School

Seoul National University

Dimethyl methylphosphonate (DMMP) is a simulant of sarin that representative of nerve agents. Sarin is an organophosphorus toxic compound that is an inhibitor of acetylcholinesterase which paralyzes human neurotransmission and autonomic nervous system. Detection of these nerve agents is important for safety from terrorism and military threats. Although there have been many studies on sensors for detecting DMMP as simulant of sarin, they still showed some limitations in specificity, sensitivity and practicality. To overcome these limitations, a human olfactory receptor (hOR)–based single–walled carbon nanotube–field effect transistor (swCNT–FET) was applied. The hOR has high specificity for certain target molecule and swCNT–FET has high sensitivity that could convert biological signal to electrical one. Through hORs screening, hOR2T7 had high selectivity for DMMP and it was produced, purified and

reconstituted for development of hOR2T7-conjugated bioelectronic nose (hOR2T7 B-nose). These hOR2T7 B-nose was able to selectively detect DMMP at a concentration of 10 fM. This shows the ultrasensitive and selective performance for the detection of DMMP as a tool for sensing CWAs, which could be used for practical application in field of safety.

**Keywords :** DMMP, chemical warfare agents, olfactory receptor, swCNT-FET, detergent micelles, bioelectronic nose

***Student Number :*** 2016-21040

# Contents

Abstract .....	i
Contents .....	iii
List of figures .....	iv
<b>1. Introduction .....</b>	<b>1</b>
1.1. Importance of sensing of Chemical warfare agents .....	1
1.2. Human olfactory receptor based bioelectronic nose .....	2
1.3. Summary of this work .....	3
<b>2. Materials and methods .....</b>	<b>4</b>
2.1. Mammalian cell culture and expression of human olfactory receptor (hORs) .....	4
2.2. Biological screening of hORs repertoire .....	5
2.3. hOR protein production, purification and reconstitution .....	6
2.4. Fabrication of single-walled carbonnanotube field-effect transistor (swCNT-FET) .....	7
2.5. Development of a bioelectronic nose for the detection of DMMP .....	8
<b>3. Result and discussion .....</b>	<b>10</b>
3.1. Screening hORs using cell-based analysis .....	10
3.2. Production of hOR2T7 in <i>E. coli</i> .....	19
3.3. Characteristics of hOR immobilized bioelectronic nose .....	22
3.4 Real-time detection of DMMP using the bioelectronic nose .....	26
<b>4. Conclusion .....</b>	<b>32</b>
<b>References .....</b>	<b>33</b>
<b>초록 .....</b>	<b>38</b>

## List of figures

<b>Figure 1.</b> Schematic representation of Human olfactory receptor (hOR) based CNT–FET sensor for detection of DMMP .....	9
<b>Figure 2.</b> Cytotoxicity analysis of DMMP .....	12
<b>Figure 3.</b> Western blot analysis of hORs expression in Hana3A cell .....	13
<b>Figure 4.</b> Response of 120 human olfactory receptors to 1 mM of DMMP ..	14
<b>Figure 5.</b> Does–dependent response curves of 4 human olfactory receptors (hOR5M10, hOR2T7, hOR8G5, hOR2AG2) strongly detecting with DMMP .....	15
<b>Figure 6.</b> Structually similar molecules with DMMP .....	16
<b>Figure 7.</b> Selectivity test of hOR5M10, hOR2T7, hOR8G5 and hOR2AG2 with DMMP and structurally similar molecules .....	17
<b>Figure 8.</b> Selectivity test of hOR5M10, hOR2T7, hOR8G5 and hOR2AG2 with DMMP, molecules with similar odor and molecule with smoky odor .....	18
<b>Figure 9.</b> SDS–page gel staining analysis and western blot analysis of produced and purified hOR2T7 protein .....	20
<b>Figure 10.</b> Tryptophan fluorecence analysis of reconstituted hOR2T7 .....	21
<b>Figure 11.</b> AFM images and height profile of bare CNT channel and CNT channel functionalized with hOR.....	23
<b>Figure 12.</b> Current–voltage curves of bare CNT channel and CNT channel functionalized with hOR.....	24
<b>Figure 13.</b> Gate profile of bare CNT channel and CNT channel functionalized	

with hOR .....	25
<b>Figure 14.</b> Real-time responses of bioelectronic nose to DMMP with variable concentration.....	28
<b>Figure 15.</b> Does-dependent response of bioelectronic nose with DMMP. Error bar, s.e.m. three replicates .....	29
<b>Figure 16.</b> Selectivity test of hOR2T7 B-nose. (a) Real-time selectivity test of hOR2T7 with structurally similar molecules using bioelectronic nose. (b) Real-time selectivity test of hOR2T7 with diverse odorants using bioelectronic nose .....	30
<b>Figure 17.</b> Interference analysis of bare CNT channel with DMMP .....	31



# 1. Introduction

## 1.1. Importance of sensing of Chemical warfare agents

Dimethyl methylphosphonate (DMMP) is a structural simulant of sarin, a chemical warfare agent (CWA) [1, 2]. CWAs are those used in chemical weapons such as sarin, soman and cyanide, while sarin and soman are among nerve agents [3]. Sarin gas is an organophosphorous toxic compound that makes acetylcholinesterase inactive in human body, making control of neurotransmitters difficult at the cholinergic synapses and paralyzing neurons in the body leading to death [4]. It is known that when exposed or inhaled 10 mg of sarin vapor for 10 min, approximately half of the exposed people will die [5].

In recent years, there have been many previous studies for the detection of CWAs, especially DMMP as simulant of sarin. Methods for sensitive and practical sensing of DMMP such as a chemical sensor [6–9], colorimetric analysis [10, 11], and microcantilever (MCL) [12] have been introduced. However, there are still several challenges such as selectivity, sensitivity, sensing condition, or complex sensing procedures.

## 1.2. Human olfactory receptor based bioelectronic nose

Many researchers have reported the bioelectronic nose using human olfactory receptors (hORs) as a tool for selective and sensitive to detect target molecule. [13, 14] The hORs expressed in human olfactory epithelium have the ability to detect sensitively only the specific target molecules in various substances. That could be combined with nanomaterials such as graphene [15], carbon–nanotube (CNT) [16], conducting polymer and polypyrrole (PPy)–nanotube [17] which could enhance sensitivity through biological signal to electrical current changes [14, 18]. Although these hOR–conjugated bioelectronic nose (hOR B–nose) has high performance in sensitivity and selectivity, there were still some issues in stability, reusability or productivity of biomaterials. [19, 20] Purified and reconstituted proteins have high stability and it could be massive produced by *Escherichia coli* (*E. coli*). This bacterial expression system has many advantages such as fast and massive production and simplicity. From this, protein based B–nose shows that it could be stable sensing of target molecules and massive production. [21, 22]

### 1.3. Summary of this work

Herein, a hOR protein-based single-walled CNT field-effect transistor (swCNT-FET) was reported for selective and sensitive detection of DMMP. In addition, hOR2T7 B-nose was able to detect DMMP in real time under mild conditions. For production of the hOR protein detecting DMMP, *E. coli* was used and its structure and functionality were also confirmed. The reconstituted hOR was immobilized on CNT channels that could amplify biological signal. Thus, when hORs with a high selectivity were combined with a highly sensitive nano-scale swCNT-FET, the hOR B-nose shows ultrasensitive and selective performance for target molecules. It will provide us with a practical and easy-to-use sensor for CWAs such as sarin.

## 2. Materials and methods

### 2.1. Mammalian cell culture and expression of human olfactory receptor (hORs)

The cells used in the experiment were Hana3A cells. Hana3A cells are derived from human embryonic kidney 293T (HEK-293T), which stably expresses RTP1L, RTP2, REEP1, and proteins to confirm the function of the olfactory receptor [23, 24]. The cells were cultured at 37°C and 5% CO<sub>2</sub> in MEM medium containing 10% fetalbovineserum (FBS) at a concentration of 100µg/mL penicillins treptomycin (SigmaAldrich,USA), 1.25µg/mL amphotericinB (SigmaAldrich,USA), 1µg/mL of puromycin (SigmaAldrich,USA) was used.

Expression of olfactory receptors was excuted by transfection with a plasmid in which olfactory receptor gene was inserted using Lipofectamine3000 (Invitrogen,USA). Olfactory receptor genes were subcloned into pcDNA3 mammalian expression vectors (Invitrogen,USA) containing humanrhodopsin (Rhotag) for expression confirmation [25].

Hana3A cells were plated in 96-well plates with cells/well for 24 h. After this, Hana3A cells were transfected with 10 ng/well of pCRE-Luc, 5 ng/well of OR, 5 ng/well of pSV40-RL, 5 ng/well of RTP1s, 2.5 ng/well of M3R for 18-24 h [26, 27]. Expression of OR on cell surface was confirmed by western blot analysis. Later 24 h after transfection, washing cell with PBS and protein inhibition cocktail. The cell was lysed by sonication (2 sec on/off, 5 min). The cells were lysed by sonicator and the supernatant was obtained by

centrifugation at 15000 g for 30 min. after boiling, sample of protein loaded into SDS-page gels and transferred to PVDF membrane (Bio-Rad, USA). The membrane was blocked by TBS with 0.1 % tween-20 (TBST) and 5 % skim milk. Primary antibody was DYKDDDDK rabbit monoclonal antibody (Cell Signaling Technology, USA) which treated to the membrane for overnight at a 1:1000 dilution in TBST with 1 % skim milk at 4°C. The membrane was washed 20 min with TBST and treated secondary antibody. Secondary antibody was goat anti-rabbit IgG-HRP (Santa Cruz, USA) which treated to the membrane for 1 h at a 1:500 dilution in TBST with 5 % skim milk at 4°C. The substrate was Lumina Forte Western HRP substrate (Merck Millipore, Germany)

## 2.2. Biological screening of hORs repertoire

The Dual-Glo Luciferase Assay System (Promega, USA) was executed to find which receptors response to target molecules. Transfection medium was replaced with diluted 1 mM odorants in CD293 (Gibco, USA) with L-glutamate after transfection 24 h later. 4 h after odorant treat, luminescence was measured with Spark 10M multimode microplate reader (Tecan, Switzerland). The measured luminescence was normalized to luciferase activity by normalization formula  $[\text{CRE/Renilla (odorant)} - \text{CRE/Renilla (negative control)}] / [\text{CRE/Renilla (positive control)} - \text{CRE/Renilla (negative control)}]$ . Negative control was obtained by treating only DMSO (dimethyl

sulfoxide, Sigma Aldrich, USA) and positive control was obtained by treating 1 M forskolin (Sigma Aldrich, USA) [28]. For odorant stimulation, each odorant was diluted in DMSO. Odorants used in selectivity test are dimethyl methylphosphonate (DMMP, Sigma Aldrich, USA), dimethyl phosphite (DMP, Sigma Aldrich, USA), diethyl phosphite (DEP, Sigma Aldrich, USA), diethyl ethylphosphonate (DEEP, Sigma Aldrich, USA), diethyl allyl phosphate (DEAP, Sigma Aldrich, USA), trimethyl phosphate (TMP, Sigma Aldrich, USA), linalool (Fluka, USA), Nerol (Fluka, USA), Amyl butyrate (Sigma Aldrich, USA), Ethyl butyrate (Sigma Aldrich, USA), Guaiacol (Sigma Aldrich, USA) for hOR activity analysis.

### **2.3. hOR protein production, purification and reconstitution**

In previous reports, GPCRs including hORs were overexpressed in *E. coli* with bacterial expression vectors [29, 30]. The pET-DEST42 vector contained hOR genes and it transformed to BL21 *E. coli* cells. The cells were incubated with LB media containing ampicillin. When OD reached 0.5, the cells were treated by IPTG (Sigma Aldrich, USA) and incubated for 4 h at 37°C. Then, the cells were lysed by sonication with 5 s on/off for 10min for 2 times and insoluble pellet after centrifugation (15,000 g, 4°C, 20 min) was solubilized in 75mL of 0.1 M tris-HCl (pH 8.0), 20 mM sodium dodecyl sulfate (SDS), 100 mM dithiothreitol (DTT), and 1 mM EDTA at 30°C, 120 rpm shaking incubator

for overnight. After solubilization, dialysis was executed by a 10K MWCO dialysis cassette (Thermo Scientific, USA) with 0.1 M sodium phosphate (pH 8.0) and 10 mM SDS. After filtering of the protein using 0.2 m bottle top filter (Thermo Scientific, USA), The protein was exposed to 5mL HisTrap HP column (GE Healthcare, USA) and eluted from the column in the buffer at 0.1 M sodium phosphate (pH 6.0) and 10 mM SDS. The purified protein that has linear form was refolded in detergent micelles which were used for refolding structure of GPCR [31–33].

## **2.4. Fabrication of single-walled carbonnanotube field-effect transistor (swCNT-FET)**

A prevalent photolithography and metal deposition method were utilized to develop a swCNT-FET device. At first, photoresist (PR, Az5214) was patterned on the SiO<sub>2</sub> wafer to make swCNT patterned channels. Then, the PR patterned wafer was placed on octadecyltrichlorosilane(OTS) solution (OTS:Hexane=1:400) for 7min. Here, OTS molecules were adsorbed on the bare surface of the patterned wafer and they formed self-assembled monolayer(SAM). The OTS patterned wafer was rinsed by acetone and ethanol to remove the PR regions. Continuously, the wafer was incubated in swCNT solution (0.05mg/mlindichlorobenzene) for 20s. In this process, swCNTs were specifically adsorbed on the exposed SiO<sub>2</sub> surface due to the hydrophobicity of

OTS. After the fabrication of swCNTchannels, drain and source electrodes (Ti/Au,10/30nm) were assembled *via* thermal evaporation method. Lastly, drain and source electrodes were passivated by PR (DNR) to keep any solution off.

## 2.5. Development of a bioelectronic nose for the detection of DMMP

0.1M PSE of 2 L in methanol was treated on a CNT-FET channel region and it was incubated at room temperature for 1 h. Then, PSE was removed by DDW and the protein of 2 L was treated on the same region at room temperature for 1 h. A moist environment was maintained during the immobilization process to prevent drying. hOR2T7 were immobilized on the CNT channel *via* the linker molecules, PSE. To monitor the electrical signal of the bioelectronic nose, a buffer zone of 20 L was formed on the channel region using detergent micelles refolding buffer. Conductance changes between the source and drain electrodes were measured using a Keithley 2636A source meter (Keithley, USA) and a MST 8000 probe station (MS Tech, South Korea).



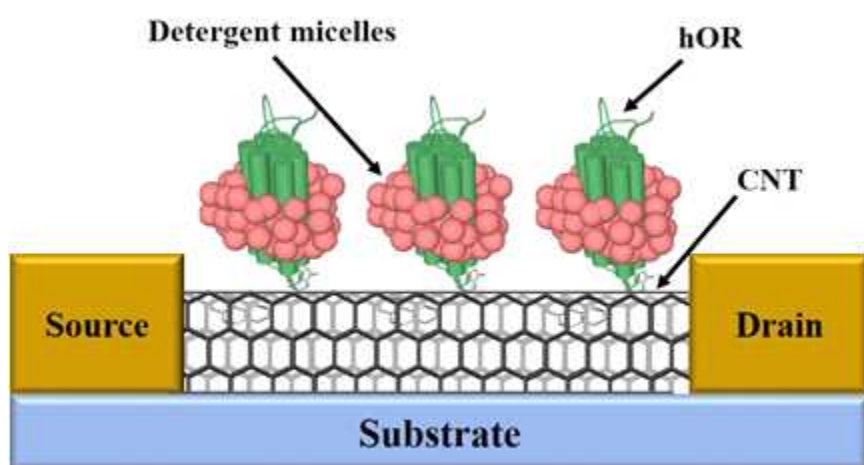


Figure 1. Schematic representation of Human olfactory receptor (hOR) based CNT-FET sensor for detection of DMMP.

## 3. Results and discussion

### 3.1. Screening hORs using cell-based analysis

Prior to screening, a cytotoxicity assay was performed to confirm the toxicity of DMMP to Hana3A cells. Fig. S1 showed that the DMMP had no influence to Hana3A cells through concentration at a 30 M to 10 mM. The result indicated that there was no interference for biological activity assay of Hana3A cells with DMMP. Through this result, screening of hORs proceeded at a 1 mM concentration that did not affect the viability of Hana3A cells and it was carried out using the luciferase assay known as a high throughput ORs screening method [24]. Fig. S2 showed that hORs expressed on Hana3A cell membrane could be confirmed by western blot analysis. In this result, the environment of human nose was successfully mimicked *in vitro*. Fig. 2a shows that seven hORs were found to be reactive with DMMP among the 120 hORs, and only four hORs were strongly reactive with DMMP. The relative response of hORs could be compared with response of each hOR through normalization formula. Also, Fig. 2b shows the normalized sensitivity from dose-dependent response of specific target molecule, DMMP at different concentration. Thorough concentration at 100M to 10 mM, responses of four hORs strongly binding with DMMP increased gradually. In this result, it was confirmed that the selected four hORs were binding to DMMP. Among the selected four hORs that strongly bound to DMMP, a selectivity test was conducted to find hORs that selectively respond to DMMP. Selectivity test was conducted in two

ways. One was to compare response of DMMP with structurally similar molecules with DMMP, and the other was to compare response of DMMP with odor similar molecules with DMMP and a smoky odor molecule that could occur in an environment where the bioelectronic nose could be used – warfare situation. DMP, DEP, DEEP, DEAP and TMP are molecules similar in structure with DMMP. Fig. S3 shows that the structure of molecules used in selectivity analysis of similar structure similar molecules. Also, linalool, nerol, amyl butyrate and ethyl butyrate are molecules with pleasant odor similar with DMMP, and guaiacol is a molecule known to have a smoky odor. Fig 2c shows that hOR2T7 had specificity to DMMP among structural similar molecules. Also, Fig 2d show that hOR2T7 had specificity to DMMP among similar odor molecules with DMMP and smoky odor molecule. Therefore, hOR2T7 selectively reacted only to DMMP, thus showing the characteristics of hOR to selectively detect DMMP. Interestingly, hOR8G5 was broadly response to molecules similar in structure with DMMP and did not respond to molecules similar in odor with DMMP and guaiacol. This suggested that hOR8G5 could show the possibility of binding to sarin, the actual target substance. Studies on olfactory receptors that broadly detect molecules that have structural similarity are under way [34, 35]. Thus, hOR8G5 could be predicted to have the characteristics of these receptors.

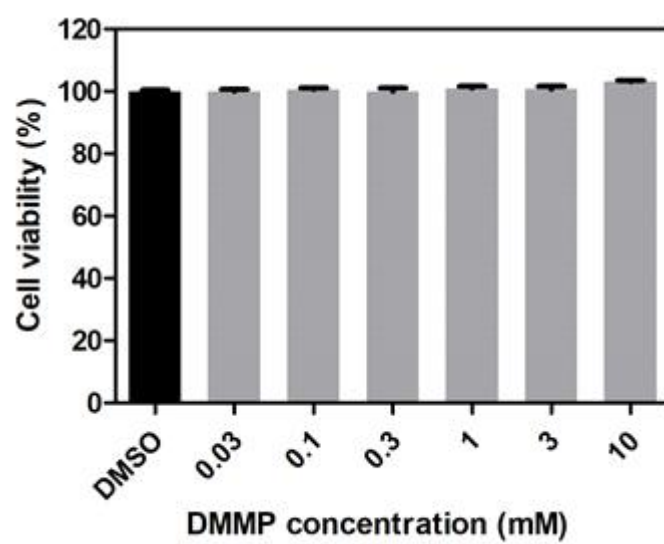


Figure 2. Cytotoxicity analysis of DMMP.

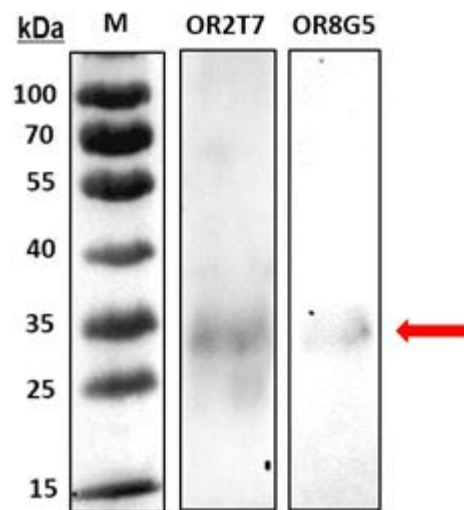


Figure 3. Western blot analysis of hORs expression in Hana3A cell.

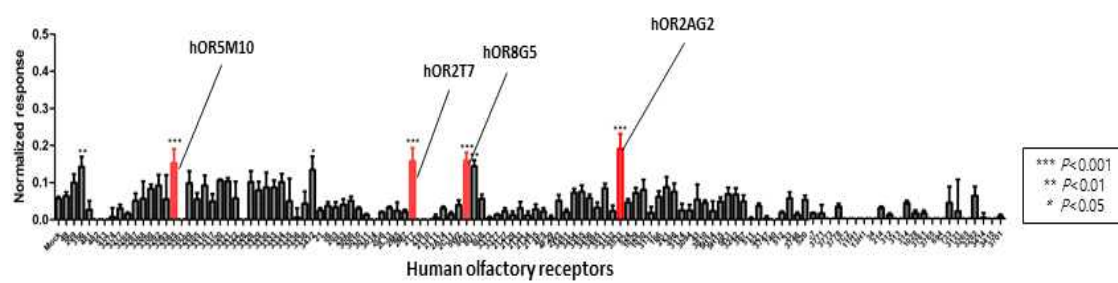


Figure 4. Response of 120 human olfactory receptors to 1 mM of DMMP.

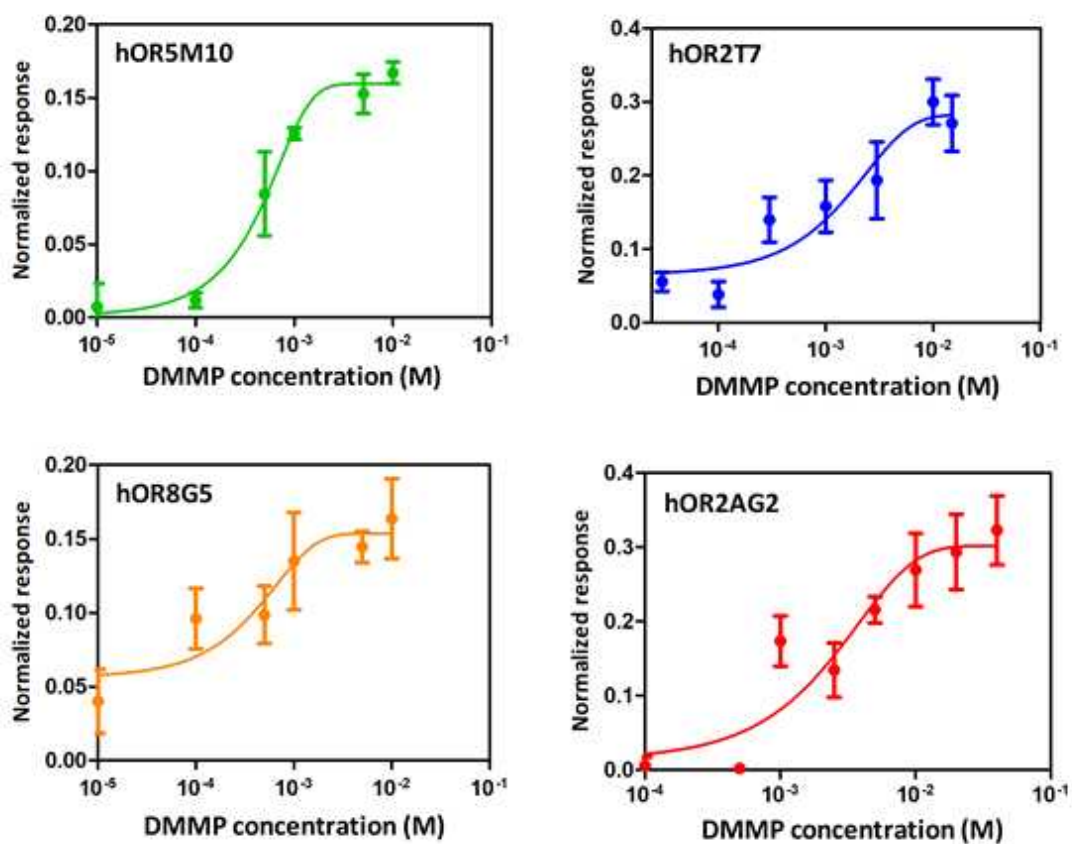


Figure 5. Does-dependent response curves of 4 human olfactory receptors (hOR5M10, hOR2T7, hOR8G5, hOR2AG2) strongly detecting with DMMP.

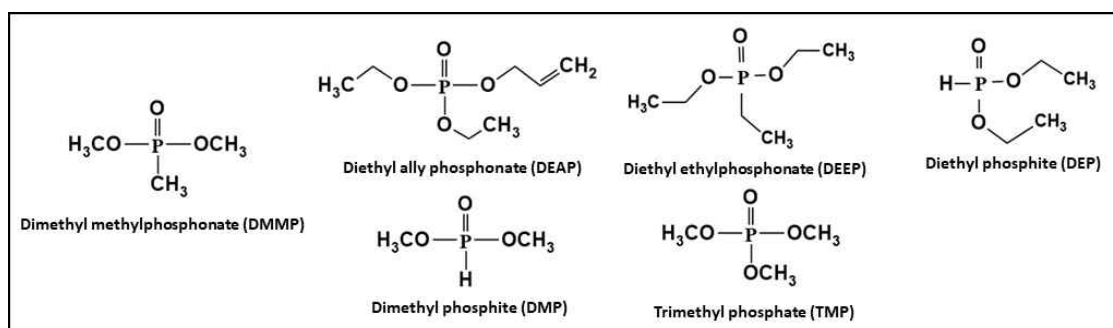


Figure 6. Structurally similar molecules with DMMP.



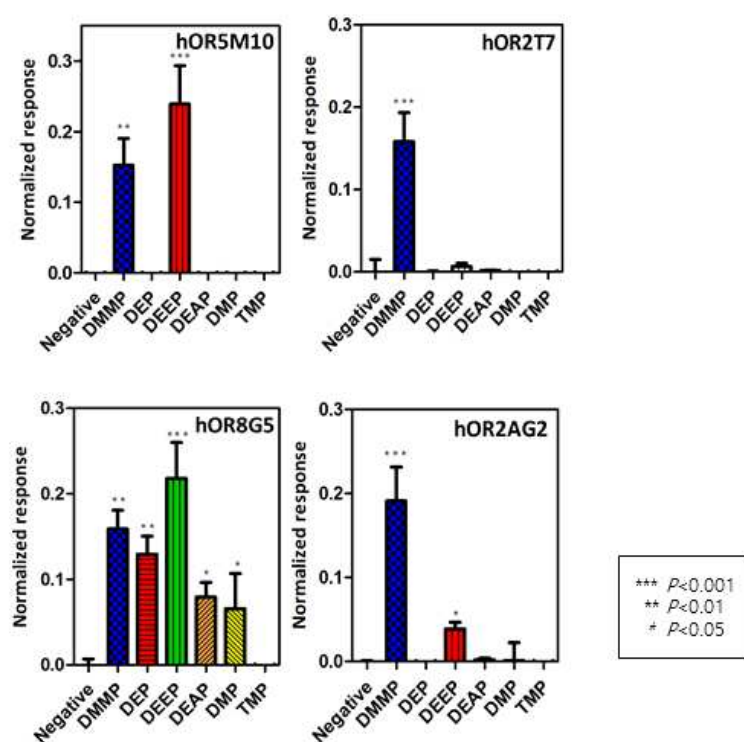


Figure 7. Selectivity test of hOR5M10, hOR2T7, hOR8G5 and hOR2AG2 with DMMP and structurally similar molecules.

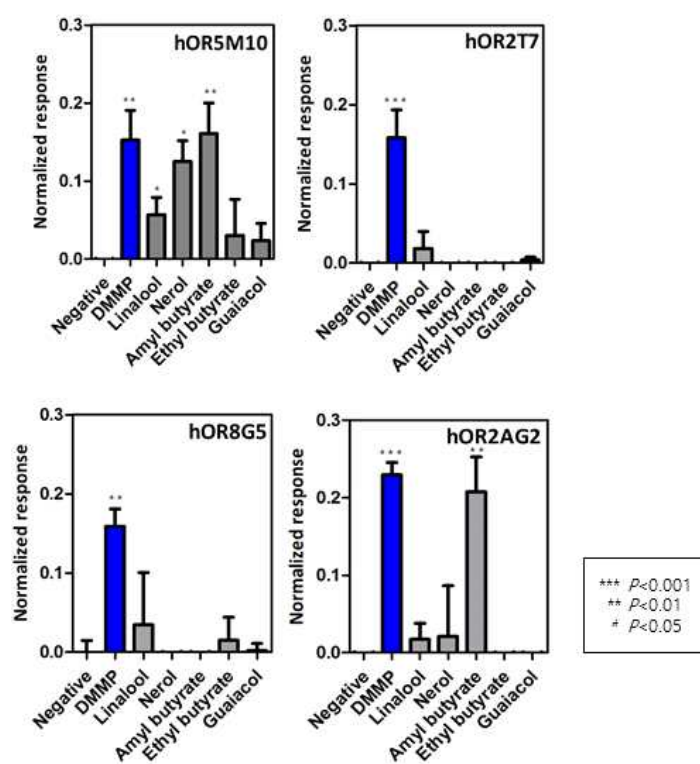


Figure 8. Selectivity test of hOR5M10, hOR2T7, hOR8G5 and hOR2AG2 with DMMP, molecules with similar odor and molecule with smoky odor.

### 3.2. Production of hOR2T7 in *E. coli*

hOR2T7 was produced from *E. coli*, purified with column chromatography and reconstituted into detergent micelles for development of protein-based sensors. Fig 3a shows the expressed and purified hOR2T7. The SDS-PAGE gel staining indicated the hOR2T7 was obtained as expected size with high purity. Also, western blot analysis was carried out by antibody against V5-tag to confirm productivity and high purity of hOR2T7. Since the protein had been denatured during purification, it was carried out a refolding process in detergent micelles to reconstitute the protein.

After reconstitution of hOR2T7, tryptophan fluorescence quenching analysis was carried out to investigate the binding property of hOR2T7. Fig. 3b shows that fluorescence of hOR2T7 was quenching gradually thorough DMMP concentration at 1 M to 20 M. When the tryptophan residues of the protein was excited at the wavelength of 280 nm, the emission was observed at the wavelength range of 340 to 350 nm [20, 36]. When DMMP was bound to hOR2T7, blocking of the tryptophan residues was occurred by changing in the structure of hOR2T7 and fluorescence intensity was quenched. Previous studies have shown that hOR2T7 has three tryptophan residues.

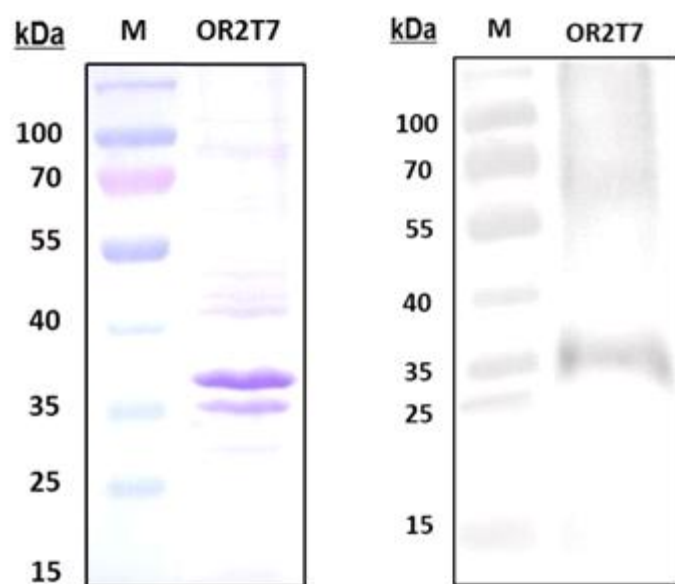


Figure 9. SDS-page gel staining analysis and western blot analysis of produced and purified hOR2T7 protein.

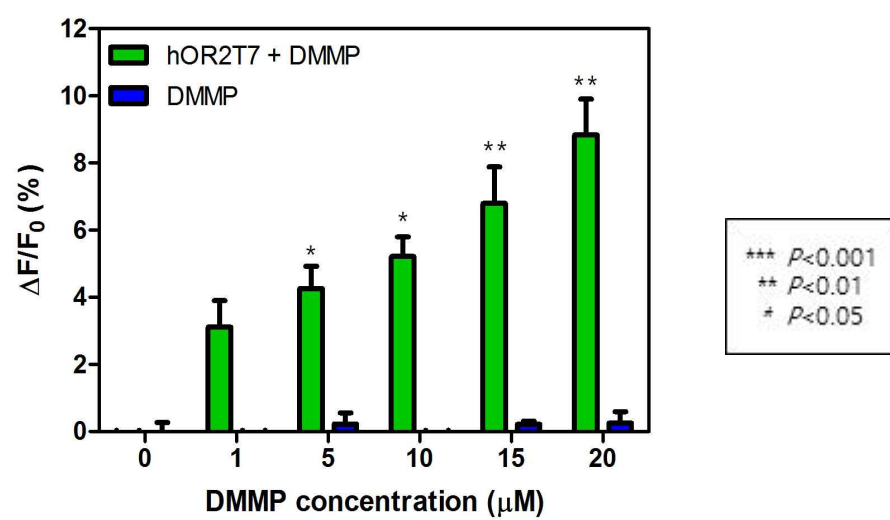


Figure 10. Tryptophan fluorescence analysis of reconstituted hOR2T7.

### 3.3. Characteristics of hOR immobilized bioelectronic nose

Fig. 3c and 3d represent the characteristics of a bioelectronics nose. Fig 3c shows atomic force microscopy (AFM) images and height profile graph to confirm the immobilization of receptor proteins on the CNT channel. They were imaged *via* a tapping mode AFM with scan rates of 0.4 and 0.1 Hz. The left and right AFM images show the swCNT surfaces before and after the immobilization of the receptor onto CNT surfaces, respectively. The height profile graph below exhibits the comparison of height profiles at the same region of the AFM images. The black and red lines in the profile graph indicate the height of swCNTs before and after immobilization of hORs on the CNT channel, respectively. The peaks of red line are higher than those of black one by 3 ~ 4 nm. These indicate that the immobilization of receptor on the CNT channel was successfully achieved. The I–V characteristics of a CNT sensor before immobilization of proteins were compared with after that on the CNT channel to confirm that function of CNT sensor remains intact even after protein immobilization. Fig. S4 shows the I–V characteristics of the sensor before and after protein immobilization, and it indicates that the electrical properties of the sensor were maintained after protein immobilization. In addition, the p-type semiconductor characteristics of the sensor could be maintained after the immobilization of proteins on the CNT surfaces (Fig. 3d). It is plausible that the decreased conductance after the immobilization was caused by the negative charge of N-terminals of protein.

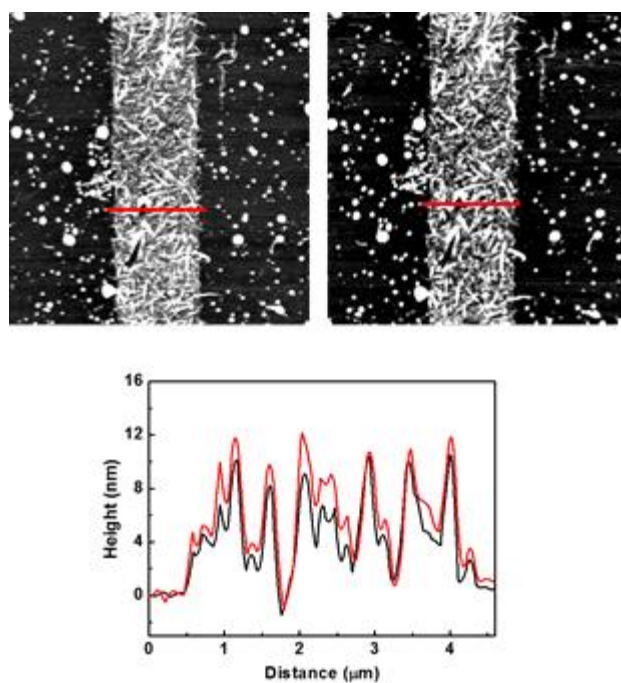


Figure 11. AFM images and height profile of bare CNT channel and CNT channel functionalized with hOR.

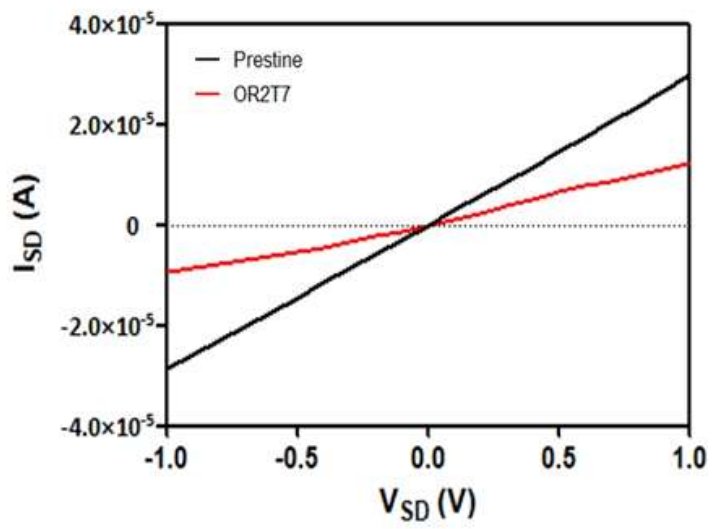


Figure 12. Current–voltage curves of bare CNT channel and CNT channel functionalized with hOR.



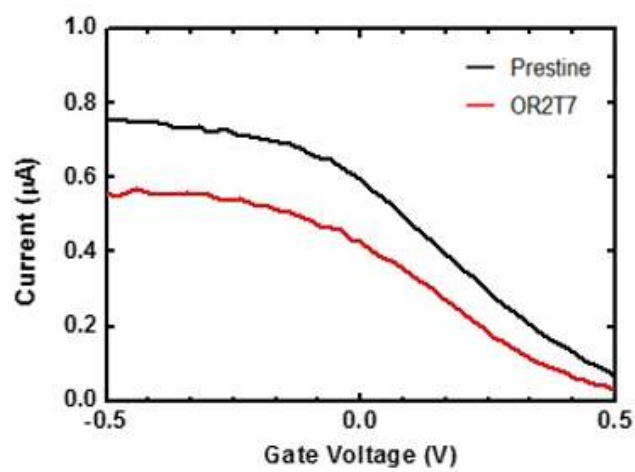


Figure 13. Gate profile of bare CNT channel and CNT channel functionalized with hOR.

### 3.4 Real-time detection of DMMP using the bioelectronic nose

Sensing measurement was performed to confirm the responses of hOR2T7 B-nose to DMMP. The responses of hOR2T7 B-nose were monitored by measuring drain-source conductance changes upon the introduction of DMMP and other molecules. Sensing processes were similar with those in previous studies [37–39], in which the binding between hOR and the ligand causes a conformational change in the hOR and it makes changes in conductance of CNT channels. [40, 41] Fig. 4a shows the real-time responses of hOR2T7 B-nose to the target molecule, DMMP, at a concentration range between 10 fM to 100 nM. The electrical conductance of hOR2T7 B-nose exhibited sharp increases after the introduction of DMMP. The responses were saturated at a concentration of 10 nM. Presumably, the conductance change of hOR2T7 B-nose can be attributed to gating effects caused by conformational change of hOR–DMMP with additional positive charges in the swCNTs. In this result, hOR2T7 B-nose could detect DMMP down to fM level, and it has a high sensitivity than any other DMMP sensor developed so far. Fig. 4b shows the normalized sensitivity of hOR2T7 B-nose to DMMP at a concentration from 1 fM to 1  $\mu$ M expressed as a calibration curve. A calibration curve was obtained by using normalization by change of drain-source conductance, that is,  $\frac{G - G_0}{G_0}$ , where the conductance when ligand was not added was  $G_0$ . Thus, the hOR2T7 B-nose showed dose-dependent responses to DMMP.

Also, Fig. 4c and 4d represent that whether selectivity of hOR2T7 remained as it was at the cellular level analysis using real-time analysis of hOR2T7

B-nose. Fig. 4c showed the selective responses of a bioelectronic nose to only DMMP among structurally similar molecules. DMP, DEP, DEAP and DEEP were used in first selectivity analysis. Fig. 4d shows that hOR2T7 B-nose also has selectivity only to DMMP among molecules with pleasant and smoky odor. Amyl butyrate, ethyl butyrate, linalool, nerol and guaiacol were used in second selectivity analysis. Each selectivity analysis was carried out at a same hOR2T7 B-nose and molecules used in analysis were added in order. In this result, hOR2T7 B-nose was able to selectively respond to DMMP. Thus, the selectivity of hOR2T7 to DMMP observed in the cell level analysis was maintained in the bioelectronic nose. For considering interference effect, the non-specific binding analysis was performed. Fig S5 showed that only swCNT-FET sensor did not response to DMMP. It shows that hOR immobilized swCNT-FETs were effectively passivated to prevent nonspecific binding with DMMP and that the hOR immobilized bioelectronic nose had reliable signals for DMMP. The newly developed sensor, called hOR2T7 B-nose, was based on high selectivity of olfactory system and sensitivity of swCNT-FET platform. hOR2T7 B-nose had ultrasensitivity and selectivity to DMMP and it was also detecting DMMP in real-time under mild condition.

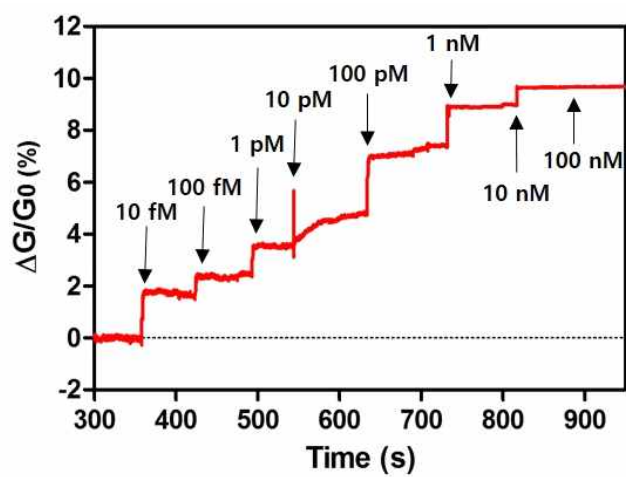


Figure 14. Real-time responses of bioelectronic nose to DMMP with variable concentration.

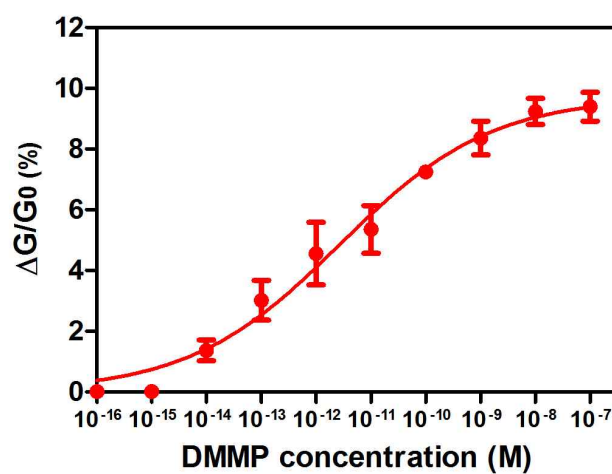


Figure 15. Dose-dependent response of bioelectronic nose with DMMP. Error bar, s.e.m. three replicates.

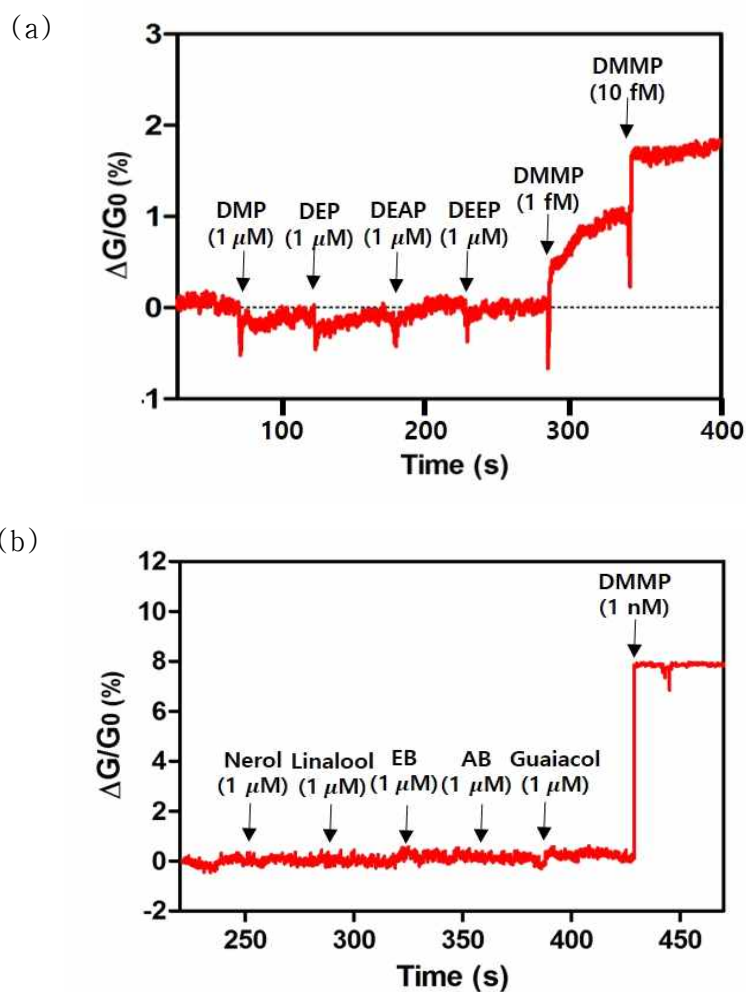


Figure 16. Selectivity test of hOR2T7 B-nose. (a) Real-time selectivity test of hOR2T7 with structurally similar molecules using bioelectronic nose. (b) Real-time selectivity test of hOR2T7 with diverse odorants using bioelectronic nose.

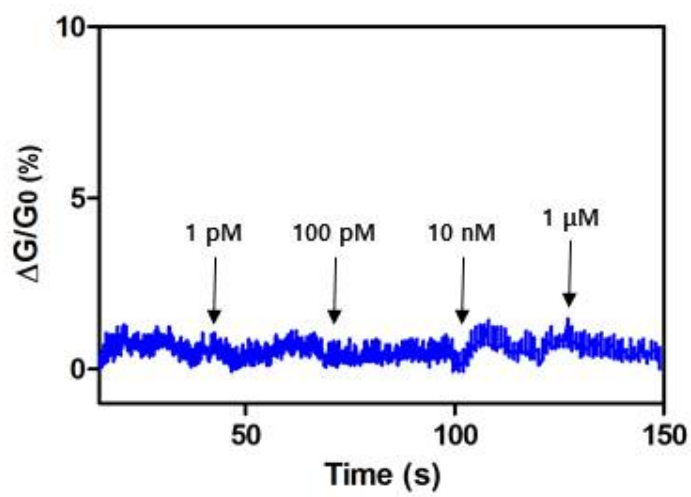


Figure 17. Interference analysis of bare CNT channel with DMMP

## 4. Conclusion

The hOR2T7 conjugated swCNT-FET sensor was developed in this research that it was sensitively and selectively detecting DMMP at a concentration of 10 fM. The hOR2T7 B-nose had not only high level of sensitivity but also the ability to detect selectively to DMMP. It was also capable of real-time detection with DMMP at mild condition. These advantages of hOR2T7 B-nose showed that it could be supplement for existing DMMP sensors which had some challenges such as sensitivity, selectivity or sensing condition.

The hOR2T7 B-nose was fabricated by placing a hOR2T7 protein on a swCNT-FET platform. It was increased stability and purity of hOR protein by producing in *E. coli* and purifying with column chromatography and reconstituting into detergent micelles. It confirmed that the reconstituted hOR2T7 protein maintained original functionality in cellular level. Electrical current measurement system with swCNT-FET platform was used for detecting DMMP and electrical signal of the bioelectronic nose could be analyzed in real-time.

In this result, hOR2T7 B-nose shows ultrasensitive and selective to DMMP. It could detect DMMP at fM range and extremely specific to DMMP at mild condition. hOR B-nose can be introduced in field of biosensors detecting CWAs such as sarin.



## 5. Reference

1. Novak, J., et al., Nerve agent detection using networks of single-walled carbon nanotubes. *Applied physics letters*, 2003. 83(19): p. 4026–4028.
2. Yoo, R., et al., Highly selective detection of dimethyl methylphosphonate (DMMP) using CuO nanoparticles/ZnO flowers heterojunction. *Sensors and Actuators B: Chemical*, 2017. 240: p. 1099–1105.
3. Wright, L.K., et al., Comparison of the lethal effects of chemical warfare nerve agents across multiple ages. *Toxicology letters*, 2016. 241: p. 167–174.
4. Bajgar, J., Organophosphates / nerve agent poisoning: mechanism of action, diagnosis, prophylaxis, and treatment. *Advances in clinical chemistry*, 2004. 38: p. 151–216.
5. Brown, M.A. and K.A. Brix, Review of health consequences from high-, intermediate-and low-level exposure to organophosphorus nerve agents. *Journal of Applied Toxicology*, 1998. 18(6): p. 393–408.
6. Kwon, O.S., et al., Carboxylic acid-functionalized conducting-polymer nanotubes as highly sensitive nerve-agent chemiresistors. *Scientific reports*, 2016. 6.
7. Šťastný, M., et al., Graphene oxide/MnO<sub>2</sub> nanocomposite as destructive adsorbent of nerve-agent simulants in aqueous media. *Applied Surface Science*, 2017. 412: p. 19–28.
8. Tomchenko, A.A., G.P. Harmer, and B.T. Marquis, Detection of chemical warfare agents using nanostructured metal oxide sensors. *Sensors and Actuators B: Chemical*, 2005. 108(1): p. 41–55.
9. Wang, F., H. Gu, and T.M. Swager, Carbon nanotube/polythiophene chemiresistive sensors for chemical warfare agents. *Journal of the*

- American Chemical Society, 2008. 130(16): p. 5392–5393.
10. Reddy, P.M., et al., Detection of cyanide ions in aqueous solutions using cost effective colorimetric sensor. *Journal of Hazardous Materials*, 2017. 334: p. 93–103.
  11. Zhou, Y., J.F. Zhang, and J. Yoon, Fluorescence and colorimetric chemosensors for fluoride-ion detection. *Chemical reviews*, 2014. 114(10): p. 5511–5571.
  12. Choi, N.-J., et al., Chemical warfare agent sensor using MEMS structure and thick film fabrication method. *Sensors and Actuators B: Chemical*, 2005. 108(1): p. 177–183.
  13. Lee, S.H., et al., Bioelectronic nose with high sensitivity and selectivity using chemically functionalized carbon nanotube combined with human olfactory receptor. *Journal of biotechnology*, 2012. 157(4): p. 467–472.
  14. Lim, J.H., et al., Nanovesicle-Based Bioelectronic Nose for the Diagnosis of Lung Cancer from Human Blood. *Advanced healthcare materials*, 2014. 3(3): p. 360–366.
  15. Park, S.J., et al., Ultrasensitive flexible graphene based field-effect transistor (FET)-type bioelectronic nose. *Nano letters*, 2012. 12(10): p. 5082–5090.
  16. Park, J., et al., A bioelectronic sensor based on canine olfactory nanovesicle-carbon nanotube hybrid structures for the fast assessment of food quality. *Analyst*, 2012. 137(14): p. 3249–3254.
  17. Yoon, H., et al., Polypyrrole nanotubes conjugated with human olfactory receptors: high-performance transducers for FET-type bioelectronic noses. *Angewandte Chemie International Edition*, 2009. 48(15): p. 2755–2758.
  18. Kim, T.H., et al., Selective and sensitive TNT sensors using biomimetic polydiacetylene-coated CNT-FETs. *ACS nano*, 2011. 5(4): p. 2824–2830.
  19. Yang, H., et al., Purification and functional reconstitution of human

- olfactory receptor expressed in *Escherichia coli*. *Biotechnology and bioprocess engineering*, 2015. 20(3): p. 423–430.
20. Kaiser, L., et al., Efficient cell-free production of olfactory receptors: detergent optimization, structure, and ligand binding analyses. *Proceedings of the National Academy of Sciences*, 2008. 105(41): p. 15726–15731.
  21. Park, S.J., et al., Dopamine Receptor D1 Agonism and Antagonism Using a Field-Effect Transistor Assay. *ACS nano*, 2017.
  22. Son, M., et al., Detection of aquaporin-4 antibody using aquaporin-4 extracellular loop-based carbon nanotube biosensor for the diagnosis of neuromyelitis optica. *Biosensors and Bioelectronics*, 2016. 78: p. 87–91.
  23. Wu, L., et al., Receptor-transporting protein 1 short (RTP1S) mediates translocation and activation of odorant receptors by acting through multiple steps. *Journal of Biological Chemistry*, 2012. 287(26): p. 22287–22294.
  24. Zhuang, H. and H. Matsunami, Evaluating cell-surface expression and measuring activation of mammalian odorant receptors in heterologous cells. *Nature protocols*, 2008. 3(9): p. 1402.
  25. Zhuang, H. and H. Matsunami, Synergism of accessory factors in functional expression of mammalian odorant receptors. *Journal of Biological Chemistry*, 2007. 282(20): p. 15284–15293.
  26. Li, Y.R. and H. Matsunami, Activation state of the M3 muscarinic acetylcholine receptor modulates mammalian odorant receptor signaling. *Science signaling*, 2011. 4(155): p. ra1.
  27. Mainland, J.D., et al., The missense of smell: functional variability in the human odorant receptor repertoire. *Nature neuroscience*, 2014. 17(1): p. 114–120.
  28. Seamon, K.B., W. Padgett, and J.W. Daly, Forskolin: unique diterpene activator of adenylate cyclase in membranes and in intact cells. *Proceedings of the National Academy of Sciences*, 1981. 78(6): p.

3363–3367.

29. Kwon, O.S., et al., Large-scale graphene micropattern nano-biohybrids: high-performance transducers for FET-type flexible fluidic HIV immunoassays. *Advanced Materials*, 2013. 25(30): p. 4177–4185.
30. Lee, S.H., et al., Mimicking the human smell sensing mechanism with an artificial nose platform. *Biomaterials*, 2012. 33(6): p. 1722–1729.
31. Ishihara, G., et al., Expression of G protein coupled receptors in a cell-free translational system using detergents and thioredoxin–fusion vectors. *Protein expression and purification*, 2005. 41(1): p. 27–37.
32. Klammt, C., et al., Evaluation of detergents for the soluble expression of  $\alpha$ -helical and  $\beta$ -barrel-type integral membrane proteins by a preparative scale individual cell-free expression system. *The FEBS journal*, 2005. 272(23): p. 6024–6038.
33. Klammt, C., et al., Cell-free expression as an emerging technique for the large scale production of integral membrane protein. *The FEBS journal*, 2006. 273(18): p. 4141–4153.
34. Charlier, L., et al., How broadly tuned olfactory receptors equally recognize their agonists. Human OR1G1 as a test case. *Cellular and molecular life sciences*, 2012. 69(24): p. 4205–4213.
35. Li, J., et al., A broadly tuned mouse odorant receptor that detects nitrotoluenes. *Journal of neurochemistry*, 2012. 121(6): p. 881–890.
36. Kiefer, H., et al., Expression of an olfactory receptor in *Escherichia coli*: purification, reconstitution, and ligand binding. *Biochemistry*, 1996. 35(50): p. 16077–16084.
37. Ahn, S.R., et al., Duplex bioelectronic tongue for sensing umami and sweet tastes based on human taste receptor nanovesicles. *ACS nano*, 2016. 10(8): p. 7287–7296.
38. Park, S.J., et al., Human dopamine receptor–conjugated multidimensional conducting polymer nanofiber membrane for dopamine detection. *ACS applied materials & interfaces*, 2016. 8(42): p. 28897–28903.

39. Son, M., et al., Bioelectronic Nose Using Odorant Binding Protein-Derived Peptide and Carbon Nanotube Field-Effect Transistor for the Assessment of Salmonella Contamination in Food. *Analytical chemistry*, 2016. 88(23): p. 11283–11287.
40. Ahn, J.H., et al., Screening of target-specific olfactory receptor and development of olfactory biosensor for the assessment of fungal contamination in grain Screening of target-specific olfactory receptor and development of olfactory biosensor for the assessment of fungal contamination in grain. *Sensors and Actuators B-Chemical*, 2015. 210: p. 9–16.
41. Kwon, O.S., et al., An Ultrasensitive, Selective, Multiplexed Superbioelectronic Nose That Mimics the Human Sense of Smell. *Nano Letters*, 2015. 15(10): p. 6559–6567.

## 요약 (국문초록)

디메틸 메틸포스포네이트 (DMMP)는 신경 작용제를 대표하는 사린의 유사 물질이다. 사린은 인간의 신경 전달 및 자율 신경계를 마비시키는 아세틸콜린 에스터레이즈의 억제제로 유기인산 화합물이다. 이러한 사린과 같은 신경 작용제의 검출은 테러와 군사적 위협으로부터의 안전을 위해 매우 중요하다. 최근에 전 세계적으로 테러에 대한 위협이 증가함에 따라 특히 사린과 같은 생화학 무기에 대한 대비가 중요해지고 있다.

사린의 유사물질인 DMMP 검출용 센서에 대해 많은 기존 연구들이 있었지만 여전히 선택도나 민감도 또는 반응조건 등에서 몇 가지 한계점을 보였다. 이러한 한계들을 극복하기 위해 인간 후각 수용체 (hOR) 기반의 탄소 나노튜브 트랜지스터 (swCNT-FET)를 개발하였다.

인간의 후각은 400여종의 후각 수용체를 기반으로 하여 후각 수용체와 냄새 물질 간의 패턴 인식을 통하여 냄새로 인식하게 된다. 이러한 후각 수용체 중에는 냄새 물질을 다양하게 감지하는 수용체도 있고 특정 냄새 물질을 선택적으로 감지하는 수용체도 있다. 일부 인간 후각수용체는 특정 물질에 대해 높은 선택도를 가지고 있으며 스크리닝 과정을 통하여 DMMP에 높은 선택도를 가진 후각 수용체를 선별하였다.

swCNT-FET는 후각 수용체의 생물학적 신호를 전기적 신호로 변환 할 수 있는 높은 민감도를 가진 센서 플랫폼이다. 이러한 플랫폼을 기반으로 한 후각 수용체 기반의 바이오 전자 코의 개발을 위하여 후각 수용체를 대장균에서 단백질로 생산, 정제하였고, detergent micelles로 구조를 형성하였다. 개발된 hOR2T7 기반의 바이오 전자코는 10 fM의 농도에서 선택적으로 DMMP를 검출 할 수 있었고, 이러한 바이오 전자코는 DMMP에 대하여 높은 민감도와 선택도를 가지는 것을 보여주었다. 개발된 바이오 전자코는 다양한 화학작용제의 감지 센서로서 여러 안전 분야에서 실제 적용되어 사용될 수 있는 가능성을 보여준다.

주요어 : DMMP, 화학 작용제, 후각 수용체, 탄소나노튜브, 바이오 전자코

학 번 : 2016-21040